

THE SLOAN DIGITAL SKY SURVEY QUASAR LENS SEARCH. II. STATISTICAL LENS SAMPLE FROM THE THIRD DATA RELEASE

NAOHISA INADA,^{1,2} MASAMUNE OGURI,^{3,4} ROBERT H. BECKER,^{5,6} MIN-SU SHIN,⁴ GORDON T. RICHARDS,⁷
 JOSEPH F. HENNAWI,⁸ RICHARD L. WHITE,⁹ BARTOSZ PINDOR,¹⁰ MICHAEL A. STRAUSS,⁴
 CHRISTOPHER S. KOCHANEK,¹¹ DAVID E. JOHNSTON,^{12,13} MICHAEL D. GREGG,^{5,6} ISSHA KAYO,¹⁴
 DANIEL EISENSTEIN,¹⁵ PATRICK B. HALL,¹⁶ FRANCISCO J. CASTANDER,¹⁷ ALEJANDRO CLOCCHIATTI,¹⁸
 SCOTT F. ANDERSON,¹⁹ DONALD P. SCHNEIDER,²⁰ DONALD G. YORK,^{21,22} ROBERT LUPTON,⁴
 KUENLEY CHIU,²³ YOZO KAWANO,¹⁴ RYAN SCRANTON,²⁴ JOSHUA A. FRIEMAN,^{22,25,26} CHARLES R. KEETON,²⁷
 TOMOKI MOROKUMA,²⁸ HANS-WALTER RIX,²⁹ EDWIN L. TURNER,⁴ SCOTT BURLES,^{30,31}
 ROBERT J. BRUNNER,³² ERIN SCOTT SHELDON,³³ NETA A. BAHCALL,⁴ AND MASATAKA FUKUGITA³⁴

Draft version October 29, 2018

ABSTRACT

We report the first results of our systematic search for strongly lensed quasars using the spectroscopically confirmed quasars in the Sloan Digital Sky Survey (SDSS). Among 46,420 quasars from the SDSS Data Release 3 ($\sim 4188 \text{ deg}^2$), we select a subsample of 22,683 quasars that are located at redshifts between 0.6 and 2.2 and are brighter than the Galactic extinction corrected *i*-band magnitude of 19.1. We identify 220 lens candidates from the quasar subsample, for which we conduct extensive and systematic follow-up observations in optical and near-infrared wavebands, in order to construct a complete lensed quasar sample at image separations between $1''$ and $20''$ and flux ratios of faint to bright lensed images larger than $10^{-0.5}$. We construct a statistical sample of 11 lensed quasars. Ten of these are galaxy-scale lenses with small image separations ($\sim 1'' - 2''$) and one is a large separation ($15''$) system which is produced by a massive cluster of galaxies, representing the first statistical sample of lensed quasars including both galaxy- and cluster-scale lenses. The Data Release 3 spectroscopic quasars contain an additional 11 lensed quasars outside the statistical sample.

Subject headings: gravitational lensing — quasars: general — cosmology: observations

¹ Cosmic Radiation Laboratory, RIKEN (The Physical and Chemical Research Organization), 2-1 Hirosawa, Wako, Saitama 351-0198, Japan.

² Institute of Astronomy, Faculty of Science, University of Tokyo, 2-21-1 Osawa, Mitaka, Tokyo 181-0015, Japan.

³ Kavli Institute for Particle Astrophysics and Cosmology, Stanford University, 2575 Sand Hill Road, Menlo Park, CA 94025.

⁴ Princeton University Observatory, Peyton Hall, Princeton, NJ 08544.

⁵ IGPP-LLNL, L-413, 7000 East Avenue, Livermore, CA 94550.

⁶ Department of Physics, University of California at Davis, 1 Shields Avenue, Davis, CA 95616.

⁷ Department of Physics, Drexel University, 3141 Chestnut Street, Philadelphia, PA 19104.

⁸ Department of Astronomy, University of California at Berkeley, 601 Campbell Hall, Berkeley, CA 94720-3411.

⁹ Space Telescope Science Institute, 3700 San Martin Drive, Baltimore, MD 21218.

¹⁰ Space Research Centre, University of Leicester.

¹¹ Department of Astronomy, The Ohio State University, Columbus, OH 43210.

¹² Jet Propulsion Laboratory, 4800 Oak Grove Drive, Pasadena CA, 91109.

¹³ California Institute of Technology, 1200 East California Blvd, Pasadena, CA 91125.

¹⁴ Department of Physics and Astrophysics, Nagoya University, Chikusa-ku, Nagoya 464-8062, Japan.

¹⁵ Steward Observatory, University of Arizona, 933 North Cherry Avenue, Tucson, AZ 85721.

¹⁶ Department of Physics and Astronomy, York University, 4700 Keele Street, Toronto, Ontario, M3J 1P3, Canada.

¹⁷ Institut d'Estudis Espacials de Catalunya/CSIC, Gran Capita 2-4, 08034 Barcelona, Spain.

¹⁸ Departamento de Astronomía y Astrofísica, Pontificia Universidad Católica de Chile, Casilla 306, Santiago 22, Chile.

¹⁹ Astronomy Department, Box 351580, University of Washington, Seattle, WA 98195.

²⁰ Department of Astronomy and Astrophysics, The Pennsylvania State University, 525 Davey Laboratory, University Park, PA 16802.

1. INTRODUCTION

Large systematic surveys of gravitationally lensed quasars are essential for various scientific applications, as shown in a recent review by Kochanek (2006). For example, lensing probabilities from large homogeneous surveys, which can be estimated from the number of lenses in a statistically well-defined sample of quasars, offer a probe of cosmological parameters. The largest ex-

²¹ Department of Astronomy and Astrophysics, The University of Chicago, 5640 South Ellis Avenue, Chicago, IL 60637.

²² Enrico Fermi Institute, The University of Chicago, 5640 South Ellis Avenue, Chicago, IL 60637.

²³ School of Physics, University of Exeter, Stocker Road, Exeter EX4 4QL, UK.

²⁴ University of Pittsburgh, Department of Physics and Astronomy, 3941 O'Hara Street, Pittsburgh, PA 15260.

²⁵ Center for Particle Astrophysics, Fermilab, P.O. Box 500, Batavia, IL 60510.

²⁶ Kavli Institute for Cosmological Physics, University of Chicago, Chicago, IL 60637.

²⁷ Department of Physics and Astronomy, Rutgers University, Piscataway, NJ 08854.

²⁸ National Astronomical Observatory, 2-21-1 Osawa, Mitaka, Tokyo 181-8588, Japan.

²⁹ Max Planck Institute for Astronomy, Koenigsstuhl 17, 69117 Heidelberg, Germany.

³⁰ Department of Physics, Massachusetts Institute of Technology, 77 Massachusetts Avenue, Cambridge, MA 02139.

³¹ Kavli Institute for Astrophysics and Space Research, Massachusetts Institute of Technology, Cambridge, MA 02139.

³² Department of Astronomy, University of Illinois, 1002 West Green Street, Urbana, IL 61801.

³³ Center for Cosmology and Particle Physics, Department of Physics, New York University, 4 Washington Place, New York, NY 10003.

³⁴ Institute for Cosmic Ray Research, University of Tokyo, 5-1-5 Kashiwa, Kashiwa, Chiba 277-8582, Japan.

isting survey, the Cosmic-Lens All Sky Survey (CLASS; Myers et al. 2003; Browne et al. 2003) contains a total of 22 lenses discovered from high-resolution imaging of over 16,000 flat spectrum radio sources. A subset of 13 lenses from 8,958 radio sources constitutes a statistically well-defined lens sample which has been used to study cosmological parameters as well as the structure of lens galaxies (e.g., Rusin & Tegmark 2001; Chae et al. 2002; Chen 2004; Chae et al. 2006; Mitchell et al. 2005). However, a drawback of radio lens surveys like CLASS is that the redshift distribution of the source population, which is a key component for statistical analyses, is poorly constrained (e.g., Muñoz et al. 2003). Thus we will benefit from complementary optical lens samples for which source populations are better understood, although the effects of absorption and emission by the lensing galaxies are larger in the optical than the radio (e.g., Falco et al. 1999). The largest existing statistical sample of optical lensed quasars is the Hubble Space Telescope snapshot survey (Maoz et al. 1993). It contains only five lenses selected from 502 bright high-redshift quasars, indicating the need for much larger optical lens samples.

Larger statistical lens samples will also allow the study of the formation of structure. Quasars can be lensed by structures on scales from individual galaxies, through groups, to clusters, and therefore the image separation distribution of strongly lensed quasars from small to large separations directly reflects the hierarchical structure formation and the effects of cooling the baryons (e.g., Kochanek & White 2001; Oguri 2006). Unfortunately, the probability of quasars strongly lensed by clusters is 1–2 orders of magnitudes smaller than that by galaxies, so we need large homogeneous surveys to study the full image separation distribution. Indeed, despite searching for them explicitly, no cluster-scale lens was discovered in the CLASS (Phillips et al. 2001).

The main purpose of the Sloan Digital Sky Survey Quasar Lens Search (SQLS; Oguri et al. 2006, hereafter Paper I) is to construct a large sample of lensed quasars in the optical. It is made possible by the large spectroscopic quasar catalog obtained from the data of the Sloan Digital Sky Survey (SDSS; York et al. 2000). Lens candidates are selected morphologically among the spectroscopically confirmed SDSS quasars. Additional lens candidates are selected by looking for companion objects to the SDSS quasars that have similar colors. Our selection algorithms have been tested against simulated SDSS images; this allows accurate quantification of the selection function (see Paper I). A number of previous strong lens discoveries (Inada et al. 2007a, and references therein) indicate the effectiveness of our candidate selection algorithm.

In this paper, we present the statistical sample of strongly lensed quasars, constructed from the SDSS Data Release 3 (DR3; Abazajian et al. 2005) spectroscopic quasar catalog (Schneider et al. 2005). Lens candidates are selected according to the algorithms presented in Paper I. We conduct extensive follow-up observations for these candidates with various facilities in order to test the hypothesis that they are lensed, and to make a complete lens sample. Cosmological constraints from this statistical sample will be reported in Paper III of this series (Oguri et al. 2007a).

The structure of this paper is as follows. We describe

the construction of the source quasar sample in §2, and the selection of lens candidates in §3. Results of our follow-up observations for the candidates are summarized in §4. Section 5 lists lensed quasars in the statistical quasar subsample as well as those included in the DR3 quasar catalog. Finally we summarize our results in §6.

2. SOURCE QUASAR SAMPLE

The SDSS is a combination of photometric and spectroscopic surveys of a quarter of the entire sky (York et al. 2000). It uses a dedicated wide-field (3° field of view) 2.5-m telescope (Gunn et al. 2006) at the Apache Point Observatory in New Mexico, USA. Photometric observations (Gunn et al. 1998; Tucker et al. 2006) consist of imaging in five broad band filters (Fukugita et al. 1996). The data are processed and analyzed automatically by the photometric pipeline (Lupton et al. 2001; Lupton 2007). Targets for spectroscopy are selected according to selection algorithms applied to the imaging data (see Richards et al. (2002) for the quasar target selection algorithm). Spectra of these targets are obtained with a multi-fiber spectrograph (wavelength range between 3800 Å and 9200 Å at a resolution of $R \sim 1800$). The astrometric accuracy of the imaging data is better than about $0.^{\prime\prime}1$ rms per coordinate (Pier et al. 2003) and photometric zeropoint errors are less than about 0.03 magnitude over the entire survey area (Hogg et al. 2001; Smith et al. 2002; Ivezić et al. 2004; Padmanabhan et al. 2007). The data release papers (Stoughton et al. 2002; Abazajian et al. 2003, 2004, 2005; Adelman-McCarthy et al. 2006, 2007) describe the contents of the SDSS data releases.

We start with a sample of 46,420 spectroscopically confirmed quasars in the SDSS DR3 quasar catalog (Schneider et al. 2005). The area covered by the spectroscopy is 4188 deg^2 . The sample contains quasars from $z = 0.08$ to 5.41 with a median redshift of 1.47. This is *not* a well-defined quasar sample for lens surveys, as it includes objects selected with a wide variety of techniques. For example, when high redshift quasar candidates ($z > 2.2$) are targeted for SDSS spectroscopy, they are required to be point sources, leading to a strong bias against selecting small separation lenses. We focus on the low redshift ($z < 2.2$) and bright ($i_{\text{cor}} < 19.1$; here i_{cor} is the Point Spread Function magnitude corrected for Galactic extinction from the maps of Schlegel et al. (1998)) quasars of the main quasar sample, which are known to have high completeness regardless of whether they are resolved or unresolved (Vanden Berk et al. 2005; Richards et al. 2006). Thus the quasars with $z < 2.2$ and $i_{\text{cor}} < 19.1$ should have no explicit biases against gravitational lenses. We further restrict the redshift range to $0.6 < z < 2.2$ to eliminate lower redshift, intrinsically extended quasars, and exclude quasars with SDSS images of poor seeing ($\text{PSF_WIDTH} > 1.^{\prime\prime}8$) in which the identification of close lens pairs is difficult. Paper I discusses the selection of the source quasars in greater detail. These criteria produce a subsample of 22,683 quasars³⁵ suitable for lens statistics. From this quasar subsample, we construct a statistical sample of lensed quasars.

³⁵ This includes one quasar (SDSS J094222.89+102025.3), which we missed in Paper I. See <http://www-utap.phys.s.u-tokyo.ac.jp/~sdss/sqls/> for the redshift and i_{cor} distributions of our quasar subsample.

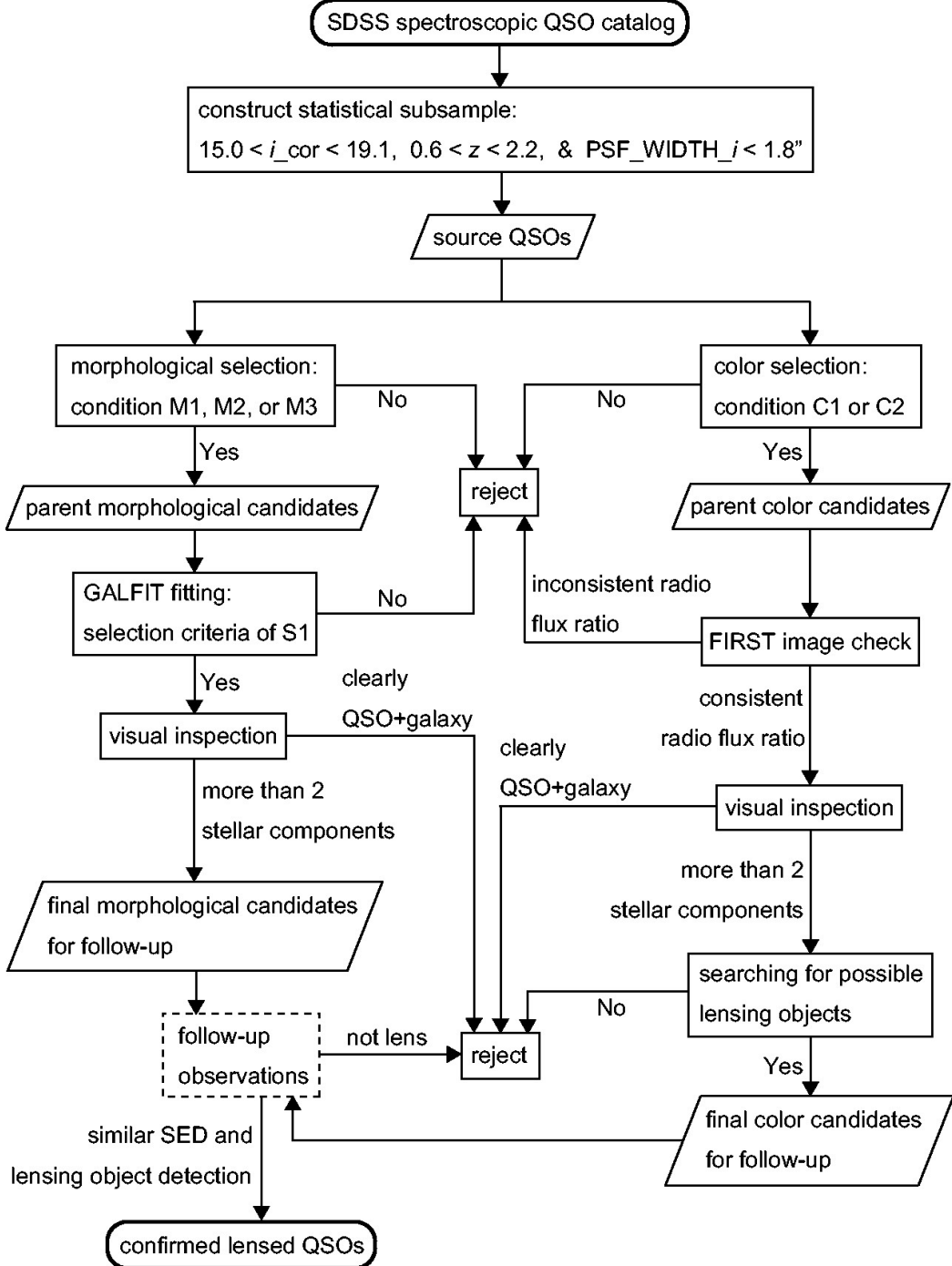


FIG. 1.— Flowchart of the candidate selection procedure of the SQLS. First we construct a statistical subsample of quasars (source QSOs) from the SDSS spectroscopic quasar catalog. The specific selection criteria (M1–M3, C1–C2, and S1) are given in Paper I. The details of the additional selection criteria are described in §3. Table 1 presents the numbers of the source quasars, parent candidates, objects rejected at each step, and final follow-up candidates.

3. LENS CANDIDATE SELECTION

We illustrate the SQLS candidate selection procedure in Figure 1. As discussed in Paper I, we use two different selection methods (morphological and color selection), in order to identify both galaxy- and cluster-scale lens candidates. For candidates selected by each approach, we apply several additional selection criteria to construct a final lens candidate sample appropriate for detailed follow-up on other facilities. We explain these additional criteria for morphological candidates in § 3.1 and those

for color candidates in § 3.2. These two selection algorithms are not exclusive with each other, since the (de-blended) quasar component of a color candidate could be a morphological candidate. The numbers of candidates selected/removed by each approach are summarized in Table 1. We finally identify 220 lensed quasar candidates for follow-up from the 22,683 source quasars.

3.1. Morphological Selection

The morphological selection algorithm is intended to discover galaxy-scale ($\theta \lesssim 2''.5$) lensed quasars that the

TABLE 1
NUMBERS OF CANDIDATES

	Number
Source quasars	22,683
Parent morphological candidates	649
Rejected by GALFIT fitting	−552
Rejected by visual inspection	−7
Final morphological candidates for follow-up	90
Parent color candidates	227
Rejected by FIRST image check	−16
Rejected by visual inspection	−16
Rejected by searching for possible lensing objects	−63
Final color candidates for follow-up	132
Final total candidates for follow-up	220

NOTE. — Two candidates are selected by both the morphological and color selection algorithms.

SDSS photometric pipeline did not deblend into multiple components. In Paper I, we showed that such lens candidates can be identified by searching for quasars that are not well fit by the PSF in each SDSS field. Thus we select the galaxy-scale lens candidates based on the goodness of fit of a quasar image to the PSF model in each field (`star_L`). Different criteria of `star_L` are used according to the object classification (`objc_type`), which is set by the difference between the PSF and model magnitudes in the SDSS data. The specific criteria (M1, M2, or M3) are given in Paper I. These “morphological selection” criteria identify 649 quasars ($\sim 3\%$ of the source quasars) as lens candidates.

As discussed in Paper I, a significant fraction of the candidates selected by the algorithm are single quasars. In addition, the candidates contain superpositions of quasars with foreground galaxies or stars. Therefore, we use two additional criteria described below in order to exclude most of these false positives before performing any subsequent observations. In the first criterion, we fit the SDSS *u*- and *i*-band images of each candidate with two PSFs using the GALFIT software (Peng et al. 2002). When a single quasar is fitted with two PSFs, the result tends to be unusual in the sense that the fitted two PSFs have a very small separation ($\ll 1''$) and similar magnitudes, or a moderate separation ($\gtrsim 1''$) and very different magnitudes. In addition, when a single quasar plus star/galaxy system is fitted with two PSFs, the results from the SDSS *u*- and *i*-band images tend to be very different because a quasar at $0.6 < z < 2.2$ is usually much bluer than either a star or a galaxy. In particular, such quasar plus star/galaxy systems may result in very large *u*-band flux ratios since the galaxy/star component tends to be very faint in *u*-band. Thus we can eliminate a significant fraction of these false positives by making cuts to the fitted separations and flux ratios (see Paper I for selection criterion S1). This procedure (“GALFIT fitting”) successfully removes $\sim 85\%$ of the candidates. Most of the rejections are single isolated quasars, but as expected, they also include several quasar-star and quasar-galaxy pairs.

For the second criterion, we inspect the SDSS images of the remaining candidates and eliminate those which appear to be chance superpositions of a quasar and a galaxy (“visual inspection”). This visual inspection eliminates about 10% of the candidates left after the GAL-

FIT modeling and yields 90 morphological (galaxy-scale) candidates that require further investigation.

3.2. Color Selection

Larger separation ($\theta \gtrsim 2''.5$) lenses created by groups or clusters of galaxies are accurately deblended by the SDSS photometric pipeline, and therefore can be selected by comparing the colors of each quasar to those of nearby objects (“color selection”). The idea is similar to the Hennawi et al. (2006) approach for finding binary quasars in the SDSS, but we modify the color selection criteria to allow for differential extinction between lensed images. These criteria are discussed in detail in Paper I, but we have slightly broadened the limits to include image separations of $\theta < 20''.1$ and *i*-band magnitude differences of $\Delta i < 1.3$, considering the typical uncertainties in the quasar positions ($0''.1$) and magnitudes (0.05) in the SDSS data. We identified 227 quasar pairs based on the criteria.

We first test the lensing hypothesis for these candidates by comparing the radio flux ratios from the Faint Images of the Radio Sky at Twenty centimeters survey (FIRST; Becker et al. 1995) with the optical flux ratios (“FIRST image check”). We eliminate 10% of the candidates with separations larger than $6''$ (set by the $\sim 5''$ resolution of the FIRST) in which one component is radio loud with a flux well above the FIRST survey limits and the other is not. Such pairs are either binary quasars or quasar-star pairs (Kochanek et al. 1999).

Next we check the SDSS images of the candidates (“visual inspection”). Since we select both point sources and extended sources as the nearby objects in the color selection stage, quasar plus galaxy systems are sometimes selected as candidates. The purpose of visual inspection in the color selection algorithm is to eliminate the candidates whose companion objects to the SDSS quasars clearly appear to be galaxies. At this step an additional $\sim 10\%$ of the candidates are excluded.

In addition, for low-redshift candidates we can search for possible lensing galaxies in the SDSS images (“searching for possible lensing objects”). To determine the criteria, we compute the expected magnitudes of the lensing objects using the halo model of Oguri (2006). Specifically, we define the magnitude limit of the lensing galaxy (or the central galaxy of the lensing cluster for a cluster-scale lens candidate) such that 99% of simulations have a lensing galaxy brighter than that magnitude limit, and compute the magnitude limit as a function of the image separation and source (quasar) redshift. In the model, halos are linked to galaxies by adopting a universal scaling relation (with scatter) between masses of halos and luminosities of galaxies. We ignore the redshift evolution of the mass-luminosity relation, which provides conservative estimates of the minimum luminosity since standard passive evolution predicts that galaxies were brighter in the past. The luminosity is converted to observed magnitude using the K-correction for elliptical galaxies in Fukugita et al. (1995). Figure 2 shows the magnitude limit as a function of image separations and quasar redshifts. We check for a lensing galaxy in the SDSS image when its expected magnitude is brighter than $i = 20.5$ (corresponding to $\sim 0.5L_*$ for a typical lens redshift); given the magnitude limit of the SDSS images, $i_{\text{lim}} \sim 21.5$, the choice should be very conservative. In

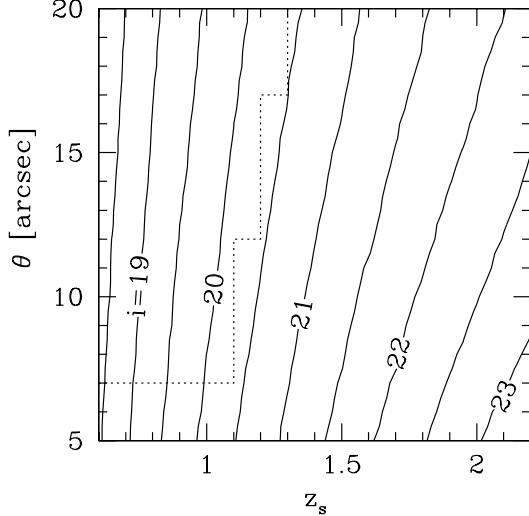


FIG. 2.— The i -band magnitude limit of the lensing objects (defined such that 99% of simulated lenses are caused by galaxies brighter than the limit) in the z_s - θ plane, where z_s denotes the source (quasar) redshift. The limit is computed using the halo model of Oguri (2006). The dotted line indicates the limits of the source redshift and image separation (eq. [1]): For candidates which lie in the region of eq. [1], we search for possible lensing galaxies in the SDSS i -band images and reject the candidates if no galaxy is seen among the components. See text for more details.

practice, we examine candidates with low redshifts and large separations defined by the region shown in Figure 2:

$$\begin{aligned} z_s < 1.1 & \quad \text{for } 7'' < \theta < 12'', \\ z_s < 1.2 & \quad \text{for } 12'' < \theta < 17'', \\ z_s < 1.3 & \quad \text{for } 17'' < \theta, \end{aligned} \quad (1)$$

where z_s is the redshift of the source quasar. The candidate which lies in the region and lacks a possible lensing object in the SDSS image is rejected. Roughly 30% of the candidates fail this test, leaving 132 color (large-separation) candidates. These 132 objects constitute the final color candidates for additional investigation. Among these, two candidates were also selected by the morphological algorithm, which is consistent with our simulation that predicts $\sim 10\%$ of objects with image separations of $1''.5 \lesssim \theta \lesssim 3''.0$ are selected by both algorithms (see Paper I). Thus the total number of candidates for follow-up is 220.

4. FOLLOW-UP OBSERVATIONS

The final morphological and color candidates and the summary of their observations are shown in Tables 2 and 3, respectively. In this section we describe the follow-up observations and how we decide on the lens nature of each candidate. We also note several interesting objects discovered in the course of our lens search.

4.1. Basic Strategy

Before conducting any subsequent observations, we first check if the candidates have been studied before with the NASA/IPAC Extragalactic Database (NED). Three of the 220 candidates are previously known gravitational lens systems for which no follow-up observations were necessary. One system, SDSS J133945.37+000946.1, turns out to be a quasar pair at different redshifts (Croom et al. 2004).

The rest of the candidates are investigated to test their lensing hypotheses. These observations consist of optical spectroscopy, optical imaging, and near-infrared imaging, conducted at the following facilities: the University of Hawaii 2.2-meter telescope (UH88), the Astrophysical Research Consortium 3.5-meter telescope (ARC 3.5-m), the Keck I and II telescopes, the United Kingdom Infra-Red Telescope (UKIRT), the Subaru telescope, the Magellan Consortium's Walter Baade 6.5-m telescope (WB 6.5-m), the Hubble Space Telescope (HST), the MDM 2.4-meter telescope (MDM 2.4-m), the MMT Observatory, the European Southern Observatory 3.6-meter telescope (ESO 3.6-m), the New Technology Telescope (NTT), and the WIYN telescope.

The SDSS images have moderate observing conditions (typically $\sim 1''.3$ seeing) and a short exposure time (about 55 sec), making it difficult in many cases to determine whether a lensing galaxy is present. Therefore, for small separation lens candidates we usually start with acquiring deeper optical (i or I) or infrared (H or K) images under good seeing conditions ($\sim 0''.5 - 1''.0$). Some of the candidates turn out to be single quasars or quasar-galaxy pairs, and therefore they are rejected rather easily. If the candidates consist of two (or more) stellar components, we take optical and/or infrared images that are deep enough to locate lensing galaxies. The typical magnitude limits for extended objects are $I \sim 23.0$, $H \sim 18.5$, and $K \sim 20.0$. Additional images with bluer filters may be taken in order to better separate multiple components. Candidates that do not exhibit any residuals after subtracting stellar components are rejected based on the absence of the lensing object. Some of our candidates are rejected simply by the fact that the separation of the two stellar components is smaller than $1''$, since we set the minimum image separation of our complete lens sample to be $1''$ (i.e., some of the “rejected” candidates with $\theta < 1''$ could in fact be gravitational lenses; see §4.2.). If the data reveal stellar components with similar colors and a possible lensing galaxy, we try to obtain spectra of the multiple stellar components to determine whether their spectral energy distributions (SEDs) are similar. We detect possible lensing objects only for 9 candidates out of 81 morphological candidates with deep images. Seven of them turn out to be new lenses from the SDSS (see § 5 and Tables 2), and the other two are confirmed to be binary quasars (SDSS J084710.40–001302.6 and SDSS J100859.55+035104.4; see § 4.2). We note that in addition to the candidates with possible lensing objects we conduct spectroscopic observations for any candidates which have stellar components with very similar colors in imaging data (including the SDSS images) even if they are rejected based on the absence of lensing objects. We perform this spectroscopic observation in order to test the validity of the rejection criterion. This includes SDSS J093207.15+072251.3 (see § 4.2) and SDSS J112012.11+671116.0 (Pindor et al. 2006) that are confirmed to be binary quasar pairs with indistinguishable redshifts.

Our strategy for follow-up of large separation lens candidates is similar to the above process. We either acquire spectra of the two components to check their SEDs or deep optical/infrared images to search for any possible lensing galaxies or clusters. Rejection based upon spectroscopic observations is straightforward

when the candidates are quasar-star pairs or quasar-quasar pairs at different redshifts. Some of the candidates turn out to be binary quasars, as reported in Hennawi et al. (2006). In some cases candidates turn out to be quasar pairs at quite similar redshifts. For these sources we use deep optical/infrared follow-up images to search for any signature of a lensing galaxy or a lensing cluster. As well as the small separation lens candidates, we perform spectroscopic observations regardless of the existences of the lensing objects particularly when the colors of the two components are very similar. Most of them are quasar-quasar pairs at different redshifts. Two of them, SDSS J090955.54+580143.2 and SDSS J211102.60+105038.3, turn out to be quasar pairs with indistinguishable redshifts, but are rejected based on the differences of the SEDs (see § 4.2).

To summarize, we identify a candidate as a lens system when the following three conditions are met: (i) the stellar components have the same redshifts within the measurement uncertainty; (ii) their SEDs are reasonably similar; (iii) a galaxy or a cluster/group of galaxies is detected between the stellar components. When candidates have four stellar images, we do not always require conditions (i) and (ii), because the object's lensing nature is obvious from its characteristic image configuration. The fact that we use the existence of the lensing object for the judgment suggests that our selection may be against hypothetical dark lenses (e.g., Rusin 2002) that have anomalously high mass-to-light ratios. However, since our candidates with very similar colors tend to be rejected spectroscopically (see above and § 4.2) rather than the absence of lensing objects alone, we believe that our follow-up strategy is reasonably effective in locating such dark lenses as well.

4.2. Notes on Individual Objects

Below we note several interesting candidates which have not been discussed elsewhere in the literature. In addition to the objects discussed below, at least 30 objects out of our 220 candidates are confirmed to be pairs of quasars; 9 out of the 30 pairs have already been reported in Hennawi et al. (2006). Furthermore, there are 9 candidates whose image separations turned out to be $\theta < 1''$ in the follow-up studies. They include the known lensed quasar FBQ1633+3134 (Morgan et al. 2001). These systems are not included in the statistical lens sample and therefore we did not perform any further spectroscopy or deeper imaging. Although our current follow-up images do not show any possible lensing objects for any of the candidates, lensing galaxies of subarcsecond lenses are expected and observed to be faint. Very deep and high resolution images are necessary to conclude whether they are lensed quasars or not. See Tables 2 and 3 for more details of these objects.

SDSS J0847–0013: This is a small separation ($\theta = 1''.0$) lens candidate discovered by the morphological selection criterion. Spectroscopic observations conducted with LRIS at Keck revealed that this is a quasar pair with similar redshifts of $z = 0.626$ and $z = 0.627$. The spectra of the two quasar components, however, have different Mg II emission line shapes (upper left panel of Figure 3), supporting the binary interpretation of this system. The image taken with Tek2k at UH88 shows extended emission in the vicinity of the brighter compo-

nent. The spectrum of this emission taken with LRIS at Keck indicates that this emission is due to the host galaxy of the quasar (Gregg et al. 2007).

SDSS J0909+5801: The spectroscopic observation at ARC 3.5-m revealed that both the components separated by $\theta = 8''.1$ are quasars at same redshifts ($z = 1.712$). However, we see a broad absorption line feature only in the C IV emission line of the brighter component (upper right panel of Figure 3). Together with the absence of the lensing object in deep *i*-band image, we conclude that the system is a binary quasar rather than a lens.

SDSS J0932+0722: A morphological candidate with an image separation of $\theta = 1''.4$ found to be a pair of quasars at $z = 1.994$ in Keck ESI observations. None of the deep optical and near-infrared images show any lensing galaxy between the two components, and the flux ratio of the two quasars in the optical are significantly different from that in the near-infrared (0.12 in *I*-band and 0.02 in *H*-band). Thus we regard this system as a binary quasar.

SDSS J1008+0351: We detected possible extended emission between the stellar components in both deep optical and infrared images. However, spectra of this small separation ($\theta = 1''.1$) candidate taken with FOCAS at Subaru suggest that this is a binary quasar, because of the slightly different redshifts ($z = 1.745$ and 1.740) and the different overall shapes of the spectra, as shown in the lower left panel of Figure 3. One interpretation is that the extended emission is due to the host galaxy of one of (or both of) the quasars.

SDSS J2111+1050: This is a large separation ($\theta = 9''.7$) lens candidate from the color selected sample. From ARC 3.5-m spectroscopy, the redshifts of the two stellar components are quite similar with $z = 1.897$. However, the SEDs (in particular, the shapes of the C IV emission lines; see the lower right panel of Figure 3) are different, and a deep *I*-band image does not show a lensing galaxy between the two components. We conclude that this is a binary quasar rather than a lens.

5. LENSED QUASARS

After completing the observations, we have a statistical sample of 11 lensed quasars with image separations of $1'' < \theta < 20''$ and *i*-band flux ratios (for two-image systems) of faint to bright lensed images larger than $10^{-0.5}$. Nine of them are newly discovered lensed quasars in the SQLS (e.g., Inada et al. 2005), and two of them, SDSS J0913+5259 (SBS 0909+523; Oscoz et al. 1997) and SDSS 1001+5553 (Q0957+561; Walsh et al. 1979), are previously known lensed quasars. The statistical sample is drawn from a subsample (22,683 quasars with $0.6 < z < 2.2$ and $i_{\text{cor}} > 19.1$) of the 46,420 DR3 quasars, and therefore some of lenses outside the SDSS DR3 (e.g., Inada et al. 2006a,b) are not included. Table 4 summarizes the DR3 statistical lensed quasar sample and Figure 4 shows a histogram of the maximum image separations of each system. The number of the lenses decreases from $\theta = 1''$ as the image separation increases, consistent with previous observations (e.g., Browne et al. 2003). The statistical sample contains 9 double lenses and 2 quadruple lenses, and ranges from $\theta = 1''.0$ to $\theta = 14''.6$, covering both galaxy- and cluster-scale lenses.

There are two lensed quasars listed in Table 2 or

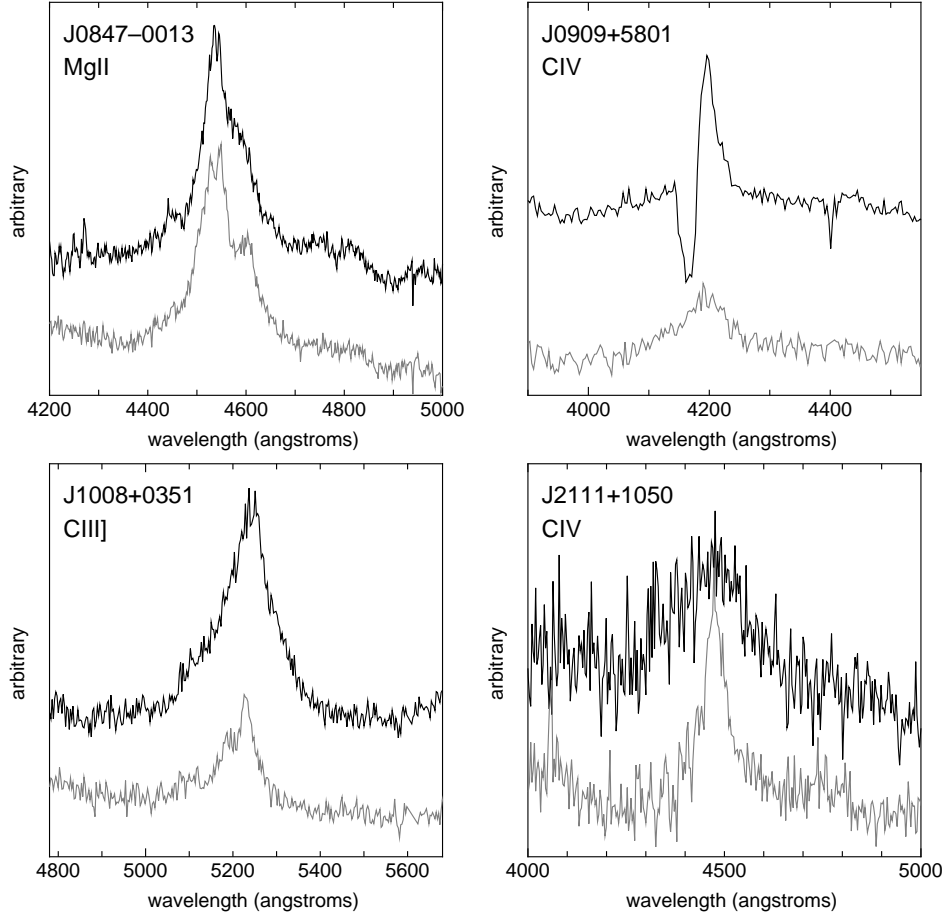


FIG. 3.— *Upper Left:* The Mg II emission lines of the two quasar components of SDSS J0847–0013 taken at the Keck telescope (spectral resolution of $R\sim 1000$). The different shapes support the binary interpretation of this system. *Upper Right:* The C IV emission lines of the two quasar components of SDSS J0909+5801 taken at the ARC 3.5-m telescope ($R\sim 500$). The broad absorption line feature is seen only in the spectrum of the brighter component, which suggests that this is a binary quasar rather than a lens. *Lower Left:* The C III] emission lines of the two quasar components of SDSS J1008+0351 from the observation at the Subaru telescope ($R\sim 500$). In addition to the different overall shapes, they show slightly different redshifts. *Lower Right:* The C IV emission lines of the two quasar components of SDSS J2111+1050 observed at the ARC 3.5-m telescope ($R\sim 500$). The different strengths of the emission lines, together with the absence of any lensing objects in the deep I -band image, support the binary interpretation.

Table 3 that are not part of our statistical sample in Table 4. SDSS J0832+0404 (Oguri et al. 2007b) is a color-selected SDSS lens but it is not included in the statistical sample because its I -band flux ratio is too extreme. The previously known lensed quasar SDSS J1633+3134 (FBQ 1633+3134; Morgan et al. 2001) is a morphologically-selected lens, but its image separation of $\theta = 0''.66$ is too small to be included in the statistical sample. These two lenses are listed in Table 5, which contains additional DR3 lensed quasars outside the statistical sample.

We also applied our selection algorithms to the DR3 spectroscopic quasars outside the subsample of 22,683 quasars. For the higher redshift quasars ($z > 2.2$), we used the `star_L` criteria for the *griz* bands rather than for the *ugri* bands of the lower redshift lens selection. We found 4 SDSS lenses, SDSS J0903+5028 (Johnston et al. 2003), SDSS J1138+0314 (Burles et al. 2007), SDSS J1155+6346 (Pindor et al. 2004), and SDSS J1406+6126 (Inada et al. 2007a), and recovered 2 known lenses, SDSS J0145–0945 (Q0142–100; Reimers et al. 2002) and SDSS J0911+0550 (RX J0911+0551; Surdej et al. 1987). Note that SDSS J0903+5028 was first identified through its

compound nature (quasar plus luminous red galaxy) of the SDSS spectrum (Johnston et al. 2003) and SDSS J1138+0314 was first identified in a WB 6.5-m snapshot survey of ~ 1000 SDSS quasars (Burles et al. 2007).

There are three lenses in the DR3 area which we did not recover as final follow-up candidate. In two cases, SDSS J0813+2545 (HS 0810+2554; Reimers et al. 2002) and SDSS J1650+4251 (Morgan et al. 2003), the objects are selected in the first stage of our morphological selection process and then eliminated by the GALFIT criteria which are designed to select lenses with $\theta > 1''$ and i -band flux ratios of faint to bright lensed images larger than $10^{-0.5}$ (see Paper I). SDSS J0813+2545 (HS 0810+2554) has a small image separation ($< 1''$) and SDSS J1650+4251 has a small flux ratio ($< 10^{-0.5}$), that is why they did not pass the GALFIT fitting. The subarcsecond ($0''.68$) radio lens (PMN J0134-0931; Winn et al. 2002; Gregg et al. 2002) was never flagged at any stage of our survey because of its small image separation. These 3 lenses would not be part of our statistical lens sample in any case. It does illustrate, however, that our survey is incomplete outside of our selection limits.

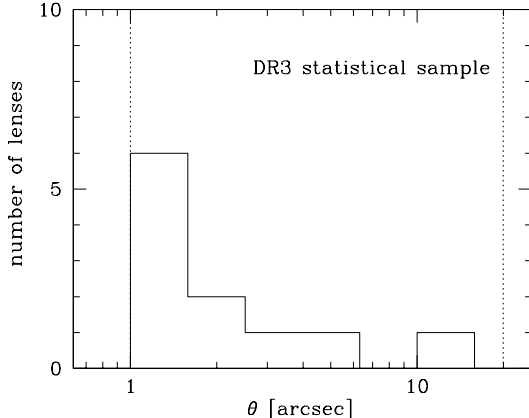


FIG. 4.— Image separation distribution of the SQLS DR3 statistical sample in bins of $\Delta \log \theta = 0.2$. The statistical sample is constructed in the range $1'' < \theta < 20''$ as indicated by the dotted lines. The individual lenses are listed in Table 4.

6. SUMMARY AND DISCUSSIONS

We have presented a complete sample of gravitationally lensed quasars which can be used for various statistical studies. The sample is based on the 46,420 spectroscopic quasars in the SDSS DR3. We focused on a subsample of 22,683 quasars with $0.6 < z < 2.2$ and Galactic extinction-corrected i -band PSF magnitudes brighter than 19.1. Lens candidates were identified using the algorithms described here and in paper I, and verified by extensive follow-up observations in the optical and near-IR. The resulting 11 lensed quasars constitute a statistical sample with image separation of $1'' < \theta < 20''$ and flux ratios (for two-image systems) of $f_i > 10^{-0.5}$ that should have very high completeness based on our tests in paper I. The DR3 spectroscopic quasar catalog contains an additional 11 lensed quasars that do not satisfy the criteria for our complete sample. Thus we identified a total of 22 lenses, 7 of which were discovered in earlier lens searches other than the SDSS.

The lens fraction in our statistical sample, $\sim 0.05\%$, appears to be lower than in previous studies, but this is largely explained by our tight criterion on the image separations and flux ratios and the fact that our sample uses relatively low-redshift faint quasars. For example, the CLASS survey found a lens fraction of $\sim 0.14\%$ (Browne et al. 2003), but $\sim 30\%$ of the lenses have separations smaller than $1''$ and $\sim 50\%$ of the double image lenses have flux ratios of faint to bright lensed images smaller than $10^{-0.5}$. The HST Snapshot Survey (Maoz et al. 1993) found that $\sim 1\%$ of bright quasars were lensed, but the magnification bias for bright quasars is significantly larger than for our fainter quasar sample.

This is the first statistical lensed quasar sample that contains both galaxy-scale ($\theta \lesssim 3''$) lenses and cluster-scale ($\theta \gtrsim 10''$) lenses. The maximum image separation in our DR3 statistical sample is $14''.62$ (SDSS J1004+4112), much larger than the maximum image separation in the CLASS, $4''.56$. The distribution of image separations across the wide mass range from galaxies to clusters will be valuable in studying the structure formation. We note that such distributions of splitting angles are obtained from surveys of lensed galaxies as well. For instance, Cabanac et al. (2007) presented 40 strongly lensed galaxy candidates, with separations ranging from $2''$ to $15''$. The simple point-like nature of source quasars,

however, makes it much easier to quantify various selection effects than in surveys of lensed galaxies. In addition, our statistical sample has an advantage over lensed galaxies (or radio lenses) in well-understood redshift distribution of the source population. As an application of the statistical sample, we study cosmological constraints from the galaxy-scale lenses of the DR3 statistical lens sample in Paper III.

The DR3 spectroscopic quasar sample consists of less than half of the full SDSS data. Our lens sample will increase significantly in the future. Assembly of a complete lens sample from the DR5 quasar catalog (Schneider et al. 2007) is in progress.

N. I. acknowledges support from the Special Postdoctoral Researcher Program of RIKEN and the Japan Society for the Promotion of Science. This work was supported in part by Department of Energy contract DE-AC02-76SF00515. A portion of this work was also performed under the auspices of the U.S. Department of Energy, National Nuclear Security Administration by the University of California, Lawrence Livermore National Laboratory under contract No. W-7405-Eng-48. M. A. S. acknowledges support from NSF grant AST 03-07409. I. K. acknowledges supports from Ministry of Education, Culture, Sports, Science, and Technology, Grant-in-Aid for Encouragement of Young Scientists (No. 17740139), and Grant-in-Aid for Scientific Research on Priority Areas No. 467 “Probing the Dark Energy through an Extremely Wide & Deep Survey with the Subaru Telescope”. A. C. acknowledges the support of CONICYT, Chile, under grant FONDECYT 1051061.

Use of the UH 2.2-m telescope and the UKIRT 3.8-m telescope for the observations is supported by the National Astronomical Observatory of Japan (NAOJ). Based in part on observations obtained with the Apache Point Observatory 3.5-meter telescope, which is owned and operated by the Astrophysical Research Consortium. Based in part on data collected at Subaru Telescope (some of data obtained from the Subaru Telescope Sciences Archive System [SMOKA]), which is operated by NAOJ. Some of the data presented herein were obtained at the W.M. Keck Observatory, which is operated as a scientific partnership among the California Institute of Technology, the University of California and the National Aeronautics and Space Administration. The Keck Observatory was made possible by the generous financial support of the W.M. Keck Foundation. The WIYN Observatory is a joint facility of the University of Wisconsin-Madison, Indiana University, Yale University, and the National Optical Astronomy Observatories. This work is also based in part on observations obtained with the MDM 2.4m Hiltner telescope, which is owned and operated by a consortium consisting of Columbia University, Dartmouth College, the University of Michigan, the Ohio State University and Ohio University. The WB 6.5-m telescope is the first telescope of the Magellan Project; a collaboration between the Observatories of the Carnegie Institution of Washington, University of Arizona, Harvard University, University of Michigan, and Massachusetts Institute of Technology to construct two 6.5 Meter optical telescopes in the southern hemisphere. Based in part on observations made with the NASA/ESA

Hubble Space Telescope, obtained at the Space Telescope Science Institute, which is operated by the Association of Universities for Research in Astronomy, Inc., under NASA contract NAS 5-26555. These observations are associated with HST program GO-9744. Based in part on observations made with telescopes (ESO 3.6-m and NTT) at the European Southern Observatories La Silla in Chile. Some observations reported here were obtained at the MMT Observatory, a joint facility of the University of Arizona and the Smithsonian Institution.

Funding for the SDSS and SDSS-II has been provided by the Alfred P. Sloan Foundation, the Participating Institutions, the National Science Foundation, the U.S. Department of Energy, the National Aeronautics and Space Administration, the Japanese Monbukagakusho, the Max Planck Society, and the Higher Education Funding Council for England. The SDSS Web Site is <http://www.sdss.org/>.

The SDSS is managed by the Astrophysical Research Consortium for the Participating Institutions. The Participating Institutions are the American Museum of Natural History, Astrophysical Institute Potsdam, University of Basel, Cambridge University, Case Western Reserve University, University of Chicago, Drexel University, Fermilab, the Institute for Advanced Study, the Japan Participation Group, Johns Hopkins University, the Joint Institute for Nuclear Astrophysics, the Kavli Institute for Particle Astrophysics and Cosmology, the Korean Scientist Group, the Chinese Academy of Sciences (LAMOST), Los Alamos National Laboratory, the Max-Planck-Institute for Astronomy (MPIA), the Max-Planck-Institute for Astrophysics (MPA), New Mexico State University, Ohio State University, University of Pittsburgh, University of Portsmouth, Princeton University, the United States Naval Observatory, and the University of Washington.

REFERENCES

- Abazajian, K., et al. 2003, AJ, 126, 2081
 Abazajian, K., et al. 2004, AJ, 128, 502
 Abazajian, K., et al. 2005, AJ, 129, 1755
 Adelman-McCarthy, J. K., et al. 2006, ApJS, 162, 38
 Adelman-McCarthy, J. K., et al. 2007, ApJS, 172, 634
 Bade, N., Siebert, J., Lopez, S., Voges, W., & Reimers, D. 1997, A&A, 317, L13
 Becker, R. H., White, R. L., & Helfand, D. J. 1995, ApJ, 450, 559
 Browne, I. W. A., et al. 2003, MNRAS, 341, 13
 Burles, S., et al. 2007, in preparation
 Cabanac, R. A., et al. 2007, A&A, 461, 813
 Chae, K.-H., et al. 2002, Phys. Rev. Lett., 89, 151301
 Chae, K.-H., Mao, S., & Kang, X. 2006, MNRAS, 373, 1369
 Chen, D.-M. 2004, A&A, 418, 387
 Croom, S. M., Smith, R. J., Boyle, B. J., Shanks, T., Miller, L., Outram, P. J., & Loaring, N. S. 2004, MNRAS, 349, 1397
 Falco, E. E., et al. 1999, ApJ, 523, 617
 Fukugita, M., Shimasaku, K., & Ichikawa, T. 1995, PASP, 107, 945
 Fukugita, M., Ichikawa, T., Gunn, J. E., Doi, M., Shimasaku, K., & Schneider, D. P. 1996, AJ, 111, 1748
 Gregg, M. D., Lacy, M., White, R. L., Glikman, E., Helfand, D., Becker, R. H., & Brotherton, M. S. 2002, ApJ, 564, 133
 Gregg, M. D., et al. 2007, in preparation
 Gunn, J. E., et al. 1998, AJ, 116, 3040
 Gunn, J. E., et al. 2006, AJ, 131, 2332
 Hennawi, J. F., et al. 2006, AJ, 131, 1
 Hogg, D. W., Finkbeiner, D. P., Schlegel, D. J., & Gunn, J. E. 2001, AJ, 122, 2129
 Inada, N., et al. 2003a, AJ, 126, 666
 Inada, N., et al. 2003b, Nature, 426, 810
 Inada, N., et al. 2005, AJ, 130, 1967
 Inada, N., et al. 2006a, AJ, 131, 1934
 Inada, N., et al. 2006b, ApJ, 653, L97
 Inada, N., et al. 2007a, AJ, 133, 206
 Inada, N., et al. 2007b, AJ, in preparation
 Ivezić, Ž., et al. 2004, AN, 325, 583
 Johnston, D. E., et al. 2003, AJ, 126, 2281
 Kochanek, C. S., Falco, E. E., & Muñoz, J. A. 1999, ApJ, 510, 590
 Kochanek, C. S. & White, M. 2001, ApJ, 559, 531
 Kochanek, C. S., Schneider, P., Wambsganss, J., 2006, Part 2 of Gravitational Lensing: Strong, Weak & Micro, Proceedings of the 33rd Saas-Fee Advanced Course, G. Meylan, P. Jetzer & P. North, eds. (Springer-Verlag: Berlin), 91
 Lupton, R., Gunn, J. E., Ivezić, Ž., Knapp, G. R., Kent, S., & Yasuda, N. 2001, in ASP Conf. Ser. 238, Astronomical Data Analysis Software and Systems X, ed. F. R. Harnden, Jr., F. A. Primini, and H. E. Payne (San Francisco: Astr. Soc. Pac.), p. 269
 Lupton, R. 2007, AJ, submitted
 Maoz, D., et al. 1993, ApJ, 409, 28
 Mitchell, J. L., Keeton, C. R., Frieman, J. A., & Sheth, R. K. 2005, ApJ, 622, 81
 Morgan, N. D., Becker, R. H., Gregg, M. D., Schechter, P. L., & White, R. L. 2001, AJ, 121, 611
 Morgan, N. D., Snyder, J. A., & Reens, L. H. 2003, AJ, 126, 2145
 Morokuma, T., et al. 2007, AJ, 133, 214
 Myers, S. T., et al. 2003, MNRAS, 341, 1
 Muñoz, J. A., Falco, E. E., Kochanek, C. S., McLeod, B. A., & Mediavilla, E. 2003, ApJ, 605, 614
 Oguri, M. 2006, MNRAS, 367, 1241
 Oguri, M., et al. 2004a, ApJ, 605, 78
 Oguri, M., et al. 2004b, PASJ, 56, 399
 Oguri, M., et al. 2005, ApJ, 622, 106
 Oguri, M., et al. 2006, AJ, 132, 999 (Paper I)
 Oguri, M., et al. 2007a, AJ, submitted (arXiv:0708.0825) (Paper III)
 Oguri, M., et al. 2007b, AJ, submitted (arXiv:0708.0871)
 Oscoz, A., Serra-Ricart, M., Mediavilla, E., Buitrago, J., & Goicoechea, L. J. 1997, ApJ, 491, L7
 Padmanabhan, N., et al. 2007, in preparation
 Peng, C. Y., Ho, L. C., Impey, C. D., & Rix, H.-W. 2002, AJ, 124, 266
 Phillips, P. M., et al. 2001, MNRAS, 328, 1001
 Pier, J. R., Munn, J. A., Hindsley, R. B., Hennessy, G. S., Kent, S. M., Lupton, R. H., & Ivezić, Ž. 2003, AJ, 125, 1559
 Pindor, B., et al. 2004, AJ, 127, 1318
 Pindor, B., et al. 2006, AJ, 131, 41
 Reimers, D., Hagen, H.-J., Baade, R., Lopez, S., & Tytler, D. 2002, A&A, 382, L26
 Richards, G. T., et al. 2002, AJ, 123, 2945
 Richards, G. T., et al. 2006, AJ, 131, 2766
 Rusin, D., & Tegmark, M. 2001, ApJ, 553, 709
 Rusin, D. 2002, ApJ, 572, 705
 Schlegel, D. J., Finkbeiner, D. P., & Davis, M. 1998, ApJ, 500, 525
 Schneider, D. P., et al. 2005, AJ, 130, 367
 Schneider, D. P., et al. 2007, AJ, 134, 102
 Smith, J. A., et al. 2002, AJ, 123, 2121
 Stoughton, C., et al. 2002, AJ, 123, 485
 Surdej, J., Swings, J.-P., Magain, P., Courvoisier, T. J.-L., & Borgeest, U. 1987, Nature, 329, 695
 Tucker, D. L., et al. 2006, AN, 327, 821
 Vanden Berk, D. E., et al. 2005, AJ, 129, 2047
 Walsh, D., Carswell, R. F., & Weymann, R. J. 1979, Nature, 279, 381
 Winn, J. N., Lovell, J. E. J., Chen, H.-W., Fletcher, A. B., Hewitt, J. N., Patnaik, A. R., & Schechter, P. L. 2002, ApJ, 564, 143
 York, D. G., et al. 2000, AJ, 120, 1579

TABLE 2
MORPHOLOGICAL CANDIDATES

Object	z^a	i_{cor}^b	θ_{SDSS}^c	Δi^c	image ^d	spec ^d	comment	Ref.
SDSS J001125.75–105710.4	0.641	18.95	0.48	0.70	UF(K)	...	single QSO	...
SDSS J004242.00+135450.0	1.622	16.72	0.56	0.81	UF(K)	...	single QSO	...
SDSS J011229.41+151213.9	1.957	18.86	1.12	0.30	WF(i)	...	QSO+galaxy	...
SDSS J012259.49+151147.2	1.276	18.17	0.45	0.36	UF(K)	...	single QSO	...
SDSS J020707.59–100541.6	0.662	18.78	0.48	0.10	UF(K)	...	single QSO	...
SDSS J021249.59+003448.7	1.222	18.86	1.69	0.73	8k(I),WF(i)	WF	QSO+galaxy	...
SDSS J021645.80–010204.8	1.087	18.55	0.53	1.35	UF(K)	...	single QSO	...
SDSS J024634.09–082536.1	1.685	17.77	1.03	1.10	AC(V, I),Ma(i),NR(K'),NM(H)	ES	SDSS Lens	1
SDSS J034601.93–070024.2	0.630	19.09	0.74	1.37	UF(K)	...	extended single QSO	...
SDSS J034801.20–070416.9	1.959	18.10	1.54	1.54	UF(K)	...	no lensing object	...
SDSS J041254.86–062049.8	1.266	18.96	0.48	0.58	UF(K)	...	single QSO	...
SDSS J072843.03+370834.9	1.404	18.97	1.34	0.08	WF(i)	...	no lensing object	...
SDSS J073406.75+273355.6	1.916	16.87	2.48	0.27	...	DA	QSO+star	...
SDSS J074352.62+245743.6	2.166	19.01	1.02	1.14	WF(i)	...	no lensing object	...
SDSS J080002.76+405927.1	1.624	19.00	0.80	1.27	8k(V)	...	single QSO	...
SDSS J083530.89+054240.7	1.696	18.50	0.99	0.18	RE(r),WF(i),QU(H)	...	no lensing object	...
SDSS J083956.19+410950.9	0.629	19.08	0.73	1.96	WF(i)	...	single QSO	...
SDSS J084512.74+543421.5	1.285	18.53	1.50	0.82	...	MS	QSO+star	2
SDSS J084710.40–001302.6	0.627	18.60	0.95	0.43	Te(I)	LR	QSO pair ($z = 0.626, 0.627$)	...
SDSS J084856.08+011540.0	0.646	18.86	1.37	0.53	Ma(i)	ES	QSO+galaxy+star	...
SDSS J085122.37+472249.0	0.894	18.80	1.47	0.03	WF(i)	...	no lensing object	...
SDSS J085643.71+413444.8	0.756	17.75	0.55	0.59	8k(V)	...	single QSO	...
SDSS J091301.03+525928.9	1.377	16.17	1.12	0.42	known lens (SBS 0909)	3
SDSS J092455.79+021924.9	1.523	18.12	1.34	0.64	Ma(u, g, r, i)	ES	SDSS Lens	4
SDSS J092528.68+071442.7	1.630	18.13	0.55	0.68	8k(V)	...	single QSO	...
SDSS J093207.15+072251.3	1.993	18.96	1.42	1.95	RE(r),8k(I),UF(K),QU(H)	ES	QSO pair ($z = 1.994, 1.994$)	...
SDSS J094945.68+632622.9	0.650	17.72	0.41	1.26	Te(I)	...	single QSO	...
SDSS J095324.39+570319.5	0.619	18.81	2.57	0.14	8k(V),Te(I)	...	no lensing object	...
SDSS J100229.46+444942.7	2.052	18.39	0.72	0.25	RE(r),Te(I),NR(K'),QU(H)	...	$\theta = 0'.$ 8	...
SDSS J100327.37+595804.0	1.138	17.71	1.19	0.09	FO(V, I)	...	no multiple point sources	...
SDSS J100859.55+035104.4	1.746	19.09	0.98	1.18	RE(r),Te(I),UF(K),QU(H)	FO	QSO pair ($z = 1.745, 1.740$)	...
SDSS J102111.02+491330.3	1.720	18.97	1.03	0.55	8k(I),NR(K')	MS	SDSS Lens	2
SDSS J103244.09+084022.5	0.604	19.05	0.87	2.05	SC(V, R)	...	single QSO	...
SDSS J104716.39+055159.5	0.891	18.51	0.54	1.50	Op(I)	...	$\theta = 0'.$ 4	...
SDSS J105337.63+074257.0	0.635	18.96	2.19	1.08	Op(I)	...	single QSO	...
SDSS J111348.65+494522.4	0.659	19.03	0.68	0.14	Op(I)	...	extended single QSO	...
SDSS J111557.64+040224.3	0.668	18.23	0.61	1.79	Op(I)	...	single QSO	...
SDSS J112012.11+671116.0	1.494	18.46	1.71	1.40	8k(I),AR(H)	MS	QSO pair ($z = 1.494, 1.494$)	2,5
SDSS J112241.58+641601.2	1.433	18.31	1.40	0.19	8k(V),Op(I)	...	no lensing object	...
SDSS J113236.06+030335.1	1.766	18.42	3.81	1.18	QU(H)	...	no lensing object	...
SDSS J113352.61+035300.5	1.780	16.90	0.41	0.92	Op(I)	...	single QSO	...
SDSS J113613.37+033840.9	1.188	18.50	1.65	0.24	...	MS	QSO+star	2
SDSS J115244.06+571202.1	1.603	17.92	0.41	1.24	8k(V)	...	single QSO	...
SDSS J121244.33+091208.1	1.686	18.63	2.04	1.37	QU(H)	EF	QSO pair ($z = 1.686, 1.600$)	...
SDSS J122558.45–005226.2	0.963	18.84	0.46	2.04	8k(V)	...	single QSO	...
SDSS J122608.02–000602.2	1.125	18.23	1.21	0.80	Ma(g, i),AC(V, I),NM(H)	DW	SDSS Lens	6
SDSS J123020.41+452047.6	2.112	18.20	0.55	1.42	8k(V)	...	single QSO	...
SDSS J123844.79+105622.2	1.305	18.54	0.97	0.92	Op(I)	...	QSO+galaxy	...
SDSS J123846.69+644836.5	1.558	17.66	1.30	1.09	8k(V),Te(I)	...	QSO+galaxy	...
SDSS J124803.09+611628.1	1.585	18.76	0.63	1.57	8k(V)	...	single QSO	...
SDSS J125141.90+031140.9	1.223	18.69	1.73	1.02	...	MS	QSO+star	2
SDSS J125617.97+584550.0	1.205	17.88	1.19	0.83	8k(V),Op(I)	...	no lensing object	...
SDSS J125758.84+623834.2	2.136	18.50	0.72	1.47	8k(V)	...	$\theta = 0'.$ 4	...
SDSS J130337.87+505824.5	2.104	18.68	1.89	1.39	8k(I)	...	QSO+galaxy	...
SDSS J131815.12+012450.6	0.688	18.04	0.41	1.15	8k(V)	...	single QSO	...
SDSS J133222.62+034739.9	1.438	17.89	0.99	0.82	SC(i),QU(H)	FO	SDSS Lens	7
SDSS J133512.10+052732.4	1.958	18.98	0.79	0.32	8k(V),Op(I)	...	$\theta = 0'.$ 8	...
SDSS J133534.79+011805.5	1.571	17.53	1.59	1.16	SC(i),NR(K')	EM	SDSS Lens	8
SDSS J133632.95+631425.0	1.799	17.21	0.58	1.98	8k(I)	...	single QSO	...
SDSS J140159.74+414156.2	1.702	17.91	1.43	2.19	QU(H)	...	QSO+galaxy+galaxy	...
SDSS J140622.44–011230.7	1.154	18.84	1.15	1.18	8k(V),Op(I)	...	no lensing object	...
SDSS J141647.60+630251.4	2.034	18.97	0.70	1.10	Op(I)	...	single QSO	...
SDSS J142011.60+003711.9	0.727	18.10	0.46	0.83	8k(I)	...	single QSO	...
SDSS J142931.58+012123.5	1.518	18.99	2.13	1.67	SC(R)	...	QSO+galaxy	...
SDSS J143239.09+510431.6	1.193	18.94	0.68	1.59	8k(V),Op(I)	...	$\theta = 0'.$ 6	...
SDSS J143826.72+642859.8	1.218	18.08	1.19	1.01	8k(I)	...	QSO+galaxy	...
SDSS J144135.56+511023.1	1.556	18.98	1.44	1.39	8k(I)	...	QSO+galaxy	...
SDSS J144654.77+610248.7	1.760	17.72	0.50	0.92	8k(V)	...	single QSO	...
SDSS J145240.53+544345.1	1.520	18.39	1.35	1.58	8k(V),Te(I)	...	QSO+galaxy	...
SDSS J145356.57–025151.8	1.740	16.40	0.41	1.71	8k(V)	...	single QSO	...
SDSS J150835.59+503820.8	0.668	18.85	0.40	1.33	8k(V)	...	single QSO	...
SDSS J151236.95+553901.0	1.361	18.92	1.96	0.89	...	MS	QSO+star	2
SDSS J151304.35+021603.8	0.637	18.42	0.57	2.09	8k(V)	...	single QSO	...
SDSS J152445.63+440949.6	1.210	18.76	1.13	0.78	Op(V, R, I)	FO	SDSS Lens	9
SDSS J154120.15+542500.6	1.654	18.40	0.70	2.15	8k(V)	...	single QSO	...

TABLE 2 — *Continued*

Object	z^a	i_{cor}^b	θ_{SDSS}^c	Δi^c	image ^d	spec ^d	comment	Ref.
SDSS J162935.01–010538.6	1.053	16.99	0.44	1.25	8k(V)	...	single QSO	...
SDSS J163348.98+313411.8	1.519	16.89	0.71	1.86	known lens (FBQ 1633)	10
SDSS J170339.54+325957.1	1.375	17.95	1.41	2.04	8k(V), Te(I)	...	QSO+galaxy	...
SDSS J171101.70+292950.9	1.329	17.84	2.18	0.71	8k(I)	...	no lensing object	...
SDSS J171117.66+584123.8	0.616	18.35	0.55	0.99	8k(V)	...	single QSO	...
SDSS J171925.07+271338.0	1.912	18.55	1.53	0.03	MM(z)	...	no lensing object	...
SDSS J172308.15+524455.5	1.818	17.14	1.02	0.88	...	MS	QSO+star	2
SDSS J211108.95+110642.3	1.003	19.00	0.62	0.03	8k(V), UF(K)	...	$\theta = 0''.6$...
SDSS J212243.01–002653.6	1.971	18.64	0.75	0.75	8k(V), UF(K)	...	$\theta = 0''.3$...
SDSS J213552.95–081048.1	0.637	19.10	0.54	0.35	8k(V)	...	single QSO	...
SDSS J213932.17–011405.7	1.232	19.03	0.49	1.05	WF(i)	...	single QSO	...
SDSS J221110.98–000953.3	0.666	18.63	0.81	1.15	UF(K)	...	$\theta = 0''.7$...
SDSS J221729.41–081154.9	1.010	18.99	0.61	2.18	UF(K)	...	single QSO	...
SDSS J231116.97–103849.7	1.540	18.79	1.81	1.43	QSO+star	2
SDSS J233713.66+005610.8	0.708	18.65	1.38	1.31	WF(i)	WF	QSO+galaxy	...

REFERENCES. — (1) Inada et al. 2005; (2) Pindor et al. 2006; (3) Oscoz et al. 1997; (4) Inada et al. 2003a; (5) Hennawi et al. 2006; (6) Inada et al. 2007b; (7) Morokuma et al. 2007; (8) Oguri et al. 2004b; (9) Oguri et al. 2007b; (10) Morgan et al. 2001.

^a Redshifts from the SDSS DR3 quasar catalog^b *i*-band PSF magnitudes with Galactic extinction corrections from the SDSS DR3 quasar catalog^c Image separations (θ_{SDSS}) in units of arcsec and magnitude differences (Δi) between the expected two components, derived from fitting the SDSS *i*-band image with two PSFs using GALFIT.^d Instruments (and filters) used for the follow-up observations. 8k: UH8k at UH88, QU: QUIRC at UH88, Op: Optic at UH88, WF: WFGS2 at UH88, Te: Tek2048 at UH88, DA: DIS III at ARC 3.5m, ES: ESI at Keck, LR: LRIS at Keck, NR: NIRC at Keck, UF: UFTI at UKIRT, FO: FOCAS at Subaru, SC: Suprime-Cam at Subaru, Ma: MagIC at WB 6.5m, DW: Double Imaging Spectrograph at WB 6.5m, AC: ACS at HST, NM: NICMOS at HST, RE: RETROCAM at MDM 2.4m, MS: MMT spectrograph, AR: ARIES at MMT, EF: EFOSC2 at ESO 3.6m, EM: EMMI at NTT, MM: MiniMo at WIYN.

TABLE 3
COLOR CANDIDATES

Object	z^a	i_{cor}^b	θ_{SDSS}^c	image ^d	spec ^d	comment	Ref.
SDSS J004757.25+144741.9	1.612	18.67	DA	QSO pair	...
SDSS J004757.87+144744.7	(2.790)	18.72	9.42	...	DA	QSO+star	...
SDSS J021649.25–003723.5	1.542	18.55	DA	QSO+star	...
SDSS J021649.15–003711.5	...	19.57	12.15	...	DA	QSO+star	...
SDSS J023205.09+010640.2	1.259	17.28	DA	QSO+star	...
SDSS J023205.18+010634.2	...	17.90	6.20	...	DA	QSO+star	...
SDSS J025804.27–001059.9	1.551	18.93	DA	different SED	...
SDSS J025803.81–001118.1	...	20.05	19.43	...	DA	different SED	...
SDSS J073118.72+371100.6	1.468	18.96	DA	QSO+star	...
SDSS J073119.02+371115.4	...	18.75	15.21	...	DA	QSO+star	...
SDSS J074013.44+292648.4	0.980	18.42	QSO pair	1
SDSS J074013.42+292645.8	(0.978)	19.68	2.64	QSO pair	1
SDSS J074357.07+300742.6	2.177	18.82	DA	QSO+star	...
SDSS J074355.82+300731.1	...	18.59	19.88	...	DA	QSO+star	...
SDSS J075011.23+430419.0	1.265	18.87	DA	QSO+star	...
SDSS J075011.66+430413.3	...	18.87	7.37	...	DA	QSO+star	...
SDSS J075310.75+292110.4	1.937	18.84	DA	QSO+star	...
SDSS J075311.03+292055.0	...	19.60	15.77	...	DA	QSO+star	...
SDSS J080435.00+314311.4	2.141	19.05	DA	different SED	...
SDSS J080435.23+314328.7	...	19.74	17.53	...	DA	different SED	...
SDSS J080658.22+273448.0	1.243	18.63	DA	no lensing object	...
SDSS J080658.17+273450.1	...	19.91	2.26	WF(i)	...	no lensing object	...
SDSS J081502.51+262804.2	1.286	18.56	DA	different SED	...
SDSS J081502.28+262804.7	...	19.53	3.11	...	DA	different SED	...
SDSS J081617.73+293639.6	0.768	18.24	DA	no lensing object	...
SDSS J081618.06+293643.7	...	19.51	5.92	UF(K)	...	no lensing object	...
SDSS J081624.72+324928.9	1.259	18.59	DA	QSO+star	...
SDSS J081624.08+324931.0	...	18.39	8.44	...	DA	QSO+star	...
SDSS J081812.94+511923.4	2.098	18.98	DA	different SED	...
SDSS J081813.02+511917.5	...	19.80	6.05	...	DA	different SED	...
SDSS J081904.56+035455.6	0.886	18.44	DA	no lensing object	...
SDSS J081904.40+035455.8	...	19.66	2.41	WF(i)	...	no lensing object	...
SDSS J082046.24+035742.1	1.574	18.57	DA	QSO pair	...
SDSS J082046.67+035740.9	(1.870)	19.13	6.44	...	DA	QSO pair	...
SDSS J083216.99+040405.2	1.115	18.89	EF	SDSS Lens	2
SDSS J083217.11+040403.8	(1.115)	19.97	2.23	Te(V, I), UF(K)	EF	SDSS Lens	2
SDSS J083349.46+440952.7	2.011	19.03	no lensing object	...
SDSS J083349.19+440954.0	...	19.89	3.17	UF(K)	...	no lensing object	...
SDSS J083557.50+341455.4	1.328	18.91	DA	QSO pair	...
SDSS J083556.32+341504.2	(1.505)	19.44	17.08	UF(K)	DA	QSO pair	...

TABLE 3 — *Continued*

Object	z^a	i_{cor}^b	θ_{SDSS}^c	image ^d	spec ^d	comment	Ref.
SDSS J083649.55+484154.0	1.710	18.04					
SDSS J083649.45+484150.0	(0.657)	19.09	4.10	QSO pair	1
SDSS J084137.51+032830.0	1.585	19.00					
SDSS J084137.75+032837.1	...	19.88	7.93	...	DA	QSO+star	...
SDSS J090809.13+444138.9	1.722	17.78					
SDSS J090809.45+444158.6	...	18.70	20.03	...	DA	QSO+star	...
SDSS J090955.54+580143.2	1.712	18.97					
SDSS J090956.50+580140.5	(1.712)	20.18	8.07	WF(<i>i</i>)	DA	QSO pair, no lensing object	...
SDSS J092024.21+030636.0	1.363	18.86					
SDSS J092024.01+030650.9	(1.450)	19.56	15.20	...	DA	QSO pair	...
SDSS J092151.55+524559.7	1.991	18.98					
SDSS J092153.00+524551.4	...	20.17	15.59	...	DA	different SED	...
SDSS J092248.35+515611.8	1.825	18.49					
SDSS J092246.22+515614.5	...	18.23	19.82	...	DA	QSO+star	...
SDSS J093336.57+620521.8	2.145	19.10					
SDSS J093336.59+620509.3	...	19.52	12.55	...	DA	QSO+star	...
SDSS J094309.66+103400.6	1.239	18.62					
SDSS J094309.36+103401.3	(1.430)	19.60	4.57	...	EF	QSO pair	...
SDSS J094510.75+472448.8	1.952	18.90					
SDSS J094510.88+472435.9	(0.560)	20.02	12.92	...	DA	QSO pair	...
SDSS J095224.84+064732.0	2.186	18.08					
SDSS J095225.25+064742.8	...	18.50	12.41	...	DA	QSO+star	...
SDSS J095711.08+640548.6	1.338	18.62					
SDSS J095711.22+640602.7	(1.288)	19.86	14.11	...	DA	QSO pair	...
SDSS J095841.15+385629.9	1.639	18.94					
SDSS J095839.67+385621.9	...	18.99	18.98	...	DA	different SED	...
SDSS J100034.17+540628.6	1.212	18.64					
SDSS J100034.86+540641.4	(1.220)	19.14	14.19	Te(<i>I</i>)	DA	QSO pair, no lensing object	...
SDSS J100120.84+555349.5	1.413	16.67					
SDSS J100120.69+555355.6	(1.405)	16.81	6.16	known lens (Q0957)	4
SDSS J100128.61+502756.8	1.839	17.31					
SDSS J100128.35+502758.4	(1.838)	17.68	2.93	8k(<i>V, R, I</i>),SP(<i>z</i>)	DA	SDSS Lens	3
SDSS J100304.55+444335.9	1.630	18.80					
SDSS J100304.61+444338.8	...	19.93	2.95	8k(<i>V, I</i>)	...	no lensing object	...
SDSS J100434.91+411242.8	1.740	18.84					
SDSS J100434.80+411239.2	(1.734)	18.41	3.76	SC(<i>g, r, i, z</i>),SP(<i>r</i>)	DA,LR	SDSS Lens (component A)	5,6
SDSS J100433.82+411234.8	(1.734)	19.34	14.71	SC(<i>g, r, i, z</i>),SP(<i>r</i>)	DA,LR	SDSS Lens (component C)	5,6
SDSS J101930.41+522411.7	1.961	18.24					
SDSS J101930.17+522413.2	...	19.47	2.70	8k(<i>V</i>),Op(<i>I</i>)	...	no lensing object	...
SDSS J103423.11+623340.3	1.406	18.76					
SDSS J103423.16+623343.3	...	19.86	3.03	8k(<i>V</i>),Op(<i>I</i>)	...	no lensing object	...
SDSS J103519.36+075258.0	1.215	19.03					
SDSS J103519.22+075256.3	(1.218)	20.11	2.66	8k(<i>I</i>),QU(<i>H</i>)	...	QSO pair, no lensing object	1
SDSS J103716.94+014126.3	1.576	19.05					
SDSS J103717.79+014121.0	...	18.68	13.95	...	DA	QSO+star	...
SDSS J103724.73+580513.0	1.517	17.39					
SDSS J103724.20+580514.1	...	17.99	4.36	...	DA	QSO+star	...
SDSS J103950.00+593511.6	1.560	18.92					
SDSS J103949.51+593505.9	...	19.72	6.81	...	DA	different SED	...
SDSS J104213.61+061942.0	1.559	18.67					
SDSS J104214.22+061959.1	(1.620)	19.60	19.41	...	DA	QSO pair	...
SDSS J104658.02+471726.9	1.532	18.58					
SDSS J104657.05+471737.4	(2.060)	19.24	14.43	...	DA	QSO pair	...
SDSS J110536.22+031952.4	0.922	18.15					
SDSS J110536.29+031955.3	...	18.92	3.06	...	DA	different SED	...
SDSS J110932.13+531635.7	0.982	18.72					
SDSS J110932.49+531635.5	(1.350)	19.00	3.25	...	DA	QSO pair	...
SDSS J112456.26+090848.8	1.649	19.03					
SDSS J112455.65+090849.7	...	19.43	9.16	Op(<i>I</i>)	...	no lensing object	...
SDSS J113813.76+024548.4	1.639	18.85					
SDSS J113814.17+024556.3	...	17.64	10.10	...	DA	QSO+star	...
SDSS J114306.19+025402.1	1.605	19.02					
SDSS J114305.85+025413.1	...	19.89	12.14	Op(<i>I</i>)	...	no lensing object	...
SDSS J114546.22+032251.9	2.008	19.01					
SDSS J114546.54+032236.7	(1.773)	19.94	15.93	QSO pair	1
SDSS J115940.79-003203.5	2.033	17.62					
SDSS J115940.40-003213.9	...	18.68	11.83	...	DA	different SED	...
SDSS J120457.12+043241.0	1.187	18.28					
SDSS J120456.64+043245.7	...	19.50	8.55	Op(<i>I</i>)	...	no lensing object	...
SDSS J120523.68-033618.2	1.495	18.80					
SDSS J120522.75-033614.6	...	17.54	14.32	...	DA	QSO+star	...
SDSS J121002.47+495312.7	1.618	18.96					
SDSS J121002.28+495253.1	(1.554)	20.06	19.74	Op(<i>I</i>)	DA	QSO pair, no lensing object	...
SDSS J121636.02+543159.2	1.894	19.01					
SDSS J121637.35+543158.2	(1.780)	20.03	11.57	...	DA	QSO pair	...

TABLE 3 — *Continued*

Object	z^a	i_{cor}^b	θ_{SDSS}^c	image ^d	spec ^d	comment	Ref.
SDSS J121647.22+495720.4	1.200	18.34					
SDSS J121647.62+495710.6	(1.195)	19.55	10.53	Op(I)	DA	QSO pair, no lensing object	...
SDSS J122126.47+572414.0	1.959	18.99					
SDSS J122126.69+572416.6	...	20.27	3.12	8k(V),Op(I)	...	no lensing object	...
SDSS J123504.17+020743.7	2.169	18.77					
SDSS J123505.16+020734.8	...	19.51	17.31	...	DA	QSO+star	...
SDSS J123558.55–023503.3	2.064	18.36					
SDSS J123558.36–023503.6	...	17.69	2.80	...	DA	QSO+star	...
SDSS J124315.47–012120.8	1.864	18.70					
SDSS J124314.68–012135.5	...	18.83	18.88	Op(I)	DA	QSO+star	...
SDSS J125029.25+025747.9	0.610	18.25					
SDSS J125028.62+025745.1	...	17.11	9.86	...	DA	QSO+star	...
SDSS J125422.00+610421.6	2.055	18.91					
SDSS J125420.54+610435.6	(2.041)	19.27	17.61	QSO pair	1
SDSS J131008.97+660350.3	1.747	18.90					
SDSS J131008.54+660349.6	...	20.04	2.74	8k(I)	...	no lensing object	...
SDSS J131505.88+590157.5	1.933	17.50					
SDSS J131507.15+590150.7	...	17.59	11.89	...	DA	QSO+star	...
SDSS J132732.66–031645.7	1.274	19.06					
SDSS J132733.00–031644.3	...	19.85	5.31	...	DA	different SED	...
SDSS J133303.35+000451.3	1.511	19.05					
SDSS J133302.65+000437.8	...	18.07	17.14	...	DA	QSO+star	...
SDSS J133945.37+000946.1	1.872	18.85					
SDSS J133945.06+001004.4	(0.978)	19.85	18.85	QSO pair, from 2dF data	7
SDSS J134702.84+032233.4	1.710	18.96					
SDSS J134703.70+032238.4	...	18.87	13.80	WF(i)	...	no lensing object	...
SDSS J134918.53–015734.8	1.586	19.09					
SDSS J134919.32–015736.9	...	19.31	12.01	Op(I)	...	no lensing object	...
SDSS J135418.26+585935.9	0.791	19.00					
SDSS J135418.10+585951.7	...	19.14	15.82	...	DA	different SED	...
SDSS J135752.15+051544.7	1.595	18.92					
SDSS J135751.03+051545.5	...	20.13	16.78	...	DA	different SED	...
SDSS J140016.87+542131.7	1.479	18.99					
SDSS J140016.19+542136.6	(1.810)	19.84	7.72	Op(I)	DA	QSO pair	...
SDSS J140326.90+561307.3	1.075	17.09					
SDSS J140326.97+561305.5	...	18.26	1.95	8k(I)	...	QSO+galaxy+galaxy	...
SDSS J142327.05+591819.8	1.672	19.06					
SDSS J142326.24+591833.5	...	18.25	15.08	...	DA	QSO+star	...
SDSS J142359.48+545250.8	1.409	18.31					
SDSS J142400.00+545248.7	(0.610)	19.56	4.94	...	DA	QSO pair	...
SDSS J142541.12+021018.7	1.665	19.04					
SDSS J142542.27+021010.1	...	19.77	19.27	Op(I)	...	no lensing object	...
SDSS J142944.25+042202.6	1.148	18.86					
SDSS J142944.18+042205.6	...	19.69	3.20	Op(I),8k(I)	...	no lensing object	...
SDSS J143433.45+613752.7	1.818	19.04					
SDSS J143432.68+613737.0	(0.427)	19.21	16.59	WF(i)	DA	QSO pair	...
SDSS J143735.94+033334.3	2.122	18.63					
SDSS J143736.44+033326.9	...	19.13	10.55	...	DA	different SED	...
SDSS J143817.62+031908.6	1.483	19.01					
SDSS J143817.02+031901.9	...	20.27	11.24	...	DA	QSO+star	...
SDSS J144104.91+044348.4	1.112	18.42					
SDSS J144104.58+044350.8	...	18.69	5.48	WF(i)	...	no lensing object	...
SDSS J144145.09+023743.0	1.160	19.07					
SDSS J144145.09+023744.8	...	19.46	1.75	...	MS	QSO+star	...
SDSS J145455.89+420306.0	1.598	19.01					
SDSS J145455.73+420256.1	...	19.60	10.04	WF(i)	DA	QSO+star	...
SDSS J150319.42+475206.8	0.757	17.92					
SDSS J150319.46+475209.7	...	18.74	2.84	8k(I)	...	no lensing object	...
SDSS J150503.46–022324.4	2.097	18.61					
SDSS J150503.70–022308.6	...	19.21	16.23	...	DA	QSO+star	...
SDSS J150533.86+013201.8	1.512	18.67					
SDSS J150534.19+013145.7	...	18.07	16.84	...	DA	QSO+star	...
SDSS J151519.40–001103.4	1.564	19.01					
SDSS J151519.94–001049.3	...	19.45	16.36	SC(I)	...	no lensing object	...
SDSS J152130.70+023915.1	2.127	18.71					
SDSS J152129.83+023917.9	...	19.08	13.33	...	DA	QSO+star	...
SDSS J152510.00+602828.1	1.337	19.03					
SDSS J152510.45+602833.3	...	19.25	6.19	Op(I)	...	no lensing object	...
SDSS J153518.78+582912.2	1.527	19.06					
SDSS J153518.86+582925.9	...	19.62	13.70	Op(I)	DA	QSO+star	...
SDSS J153559.97+430819.0	1.620	18.67					
SDSS J153559.26+430833.1	...	18.57	16.01	...	DA	QSO+star	...
SDSS J154107.47–003716.0	0.755	17.57					
SDSS J154107.21–003711.8	...	18.07	5.65	...	MS	QSO+star	8
SDSS J154148.81+523051.9	2.054	19.01					

TABLE 3 — *Continued*

Object	z^a	i_{cor}^b	θ_{SDSS}^c	image ^d	spec ^d	comment	Ref.
SDSS J154148.93+523053.6	...	19.59	1.94	8k(<i>I</i>)	...	no lensing object	...
SDSS J155723.93+492607.5	2.195	18.42					
SDSS J155723.79+492551.1	...	19.69	16.46	...	DA	different SED	...
SDSS J160305.94+272100.9	1.620	18.14					
SDSS J160307.00+272059.3	...	18.43	14.21	...	DA	QSO+star	...
SDSS J160547.59+511330.2	1.785	19.09					
SDSS J160546.66+511322.6	(1.844)	18.46	11.63	QSO pair	1
SDSS J160914.86+380728.1	1.126	18.64					
SDSS J160914.85+380730.0	...	18.68	1.93	8k(<i>I</i>)	...	no lensing object	...
SDSS J161953.24+351321.8	1.901	18.64					
SDSS J161953.45+351323.5	...	19.50	3.13	8k(<i>I</i>)	...	no lensing object	...
SDSS J161952.82+351315.4	...	19.89	8.20	8k(<i>I</i>)	...	no lensing object	...
SDSS J162602.40+334030.0	1.541	18.77					
SDSS J162603.61+334025.9	...	19.97	15.65	WF(<i>i</i>)	...	no lensing object	...
SDSS J162902.59+372430.8	0.926	19.03					
SDSS J162902.63+372435.1	(0.906)	19.37	4.35	NR(<i>K'</i>)	...	QSO pair, no lensing object	1
SDSS J165248.93+352134.1	1.498	18.33					
SDSS J165250.29+352141.6	...	19.20	18.26	WF(<i>i</i>)	...	no lensing object	...
SDSS J165459.71+305208.3	1.971	19.08					
SDSS J165459.12+305158.5	...	19.41	12.36	...	DA	QSO+star	...
SDSS J171334.41+553050.3	1.276	18.54					
SDSS J171335.03+553047.9	...	18.59	5.84	...	DA	QSO+star	...
SDSS J172633.52+530300.4	0.654	19.00					
SDSS J172633.44+530302.0	...	19.07	1.70	8k(<i>I</i>)	...	no lensing object	...
SDSS J172806.78+582039.2	2.011	19.06					
SDSS J172808.74+582040.0	...	20.17	15.46	WF(<i>i</i>)	DA	QSO+star	...
SDSS J203845.35+005532.1	1.903	18.53					
SDSS J203846.08+005541.4	...	19.47	14.32	WF(<i>i</i>)	DA	no lensing object, different SED	...
SDSS J203955.67-054102.8	1.460	18.90					
SDSS J203955.63-054044.7	...	19.80	18.08	WF(<i>i</i>)	...	no lensing object	...
SDSS J204030.52-003015.9	1.549	18.84					
SDSS J204030.71-003010.5	...	18.33	6.04	WF(<i>i</i>)	...	no lensing object	...
SDSS J204113.41-060158.5	1.432	18.63					
SDSS J204114.12-060149.0	0.830	19.56	14.19	Op(<i>I</i>)	DA	QSO pair	...
SDSS J210706.22-062506.7	1.577	18.91					
SDSS J210706.31-062503.2	...	19.56	3.71	WF(<i>i</i>)	...	no lensing object	...
SDSS J210946.73+105601.0	1.628	18.57					
SDSS J210946.23+105559.5	...	18.39	7.53	...	DA	QSO+star	...
SDSS J211102.60+105038.3	1.897	18.87					
SDSS J211102.41+105047.5	(1.897)	19.02	9.67	Te(<i>I</i>)	DA	QSO pair (different SED)	...
SDSS J211230.33-063332.1	1.554	18.94					
SDSS J211229.31-063331.4	(0.551)	19.71	15.21	QSO pair	1
SDSS J211610.83+111429.0	1.076	18.46					
SDSS J211610.58+111423.2	...	19.23	6.83	...	DA	different SED	...
SDSS J212429.88-004727.0	1.614	18.96					
SDSS J212430.90-004725.2	...	19.11	16.26	...	DA	different SED	...
SDSS J212906.23-071613.3	1.213	18.57					
SDSS J212906.32-071612.1	...	17.81	1.79	QSO+star	8
SDSS J212956.44-005150.4	1.112	18.98					
SDSS J212956.56-005152.4	...	20.04	2.68	WF(<i>i</i>)	...	no lensing object	...
SDSS J213414.01-004533.1	1.535	18.77					
SDSS J213414.17-004514.6	...	18.44	18.59	...	DA	different SED	...
SDSS J213639.11+114731.8	1.518	19.04					
SDSS J213640.40+114736.9	...	18.13	19.47	...	DA	different SED	...
SDSS J220256.32-092556.7	0.723	18.31					
SDSS J220257.01-092602.3	...	18.80	11.71	...	DA	different SED	...
SDSS J222504.14+123814.5	1.549	19.04					
SDSS J222503.32+123815.1	...	18.15	12.08	...	DA	QSO+star	...
SDSS J222822.17-005943.5	2.172	18.62					
SDSS J222822.18-005949.3	...	19.14	5.82	...	DA	QSO+star	...
SDSS J223219.23+140017.0	0.725	18.87					
SDSS J223219.42+140012.6	...	19.06	5.16	...	DA	QSO+star	...
SDSS J230250.85+143203.2	0.654	18.99					
SDSS J230250.90+143158.5	...	20.17	4.71	...	DA	different SED	...
SDSS J230951.18-094016.3	1.572	19.07					
SDSS J230950.59-093958.3	...	20.32	20.04	...	DA	different SED	...
SDSS J231152.83+145455.0	1.261	18.98					
SDSS J231152.38+145507.5	...	19.88	14.17	QSO+star	1
SDSS J235108.66+134322.6	1.218	18.81					
SDSS J235108.70+134320.8	...	19.92	1.86	WF(<i>i</i>)	...	no lensing object	...
SDSS J235924.73+152541.6	1.574	19.01					
SDSS J235924.84+152544.3	...	19.98	3.09	WF(<i>i</i>)	...	no lensing object	...

TABLE 3 — *Continued*

Object	z^a	i_{cor}^b	θ_{SDSS}^c	image ^d	spec ^d	comment	Ref.
REFERENCES. — (1) Hennawi et al. 2006; (2) Oguri et al. 2007b; (3) Oguri et al. 2005; (4) Walsh et al. 1979; (5) Inada et al. 2003b; (6) Oguri et al. 2004a; (7) Croom et al. 2004; (8) Pindor et al. 2006.							

NOTE. — Two candidates that are identified by the morphological selection algorithm as well, SDSS J073406.75+273355.6 and SDSS J133534.79+011805.5, are listed in Table 2.

^a Redshifts from the SDSS DR3 quasar catalog and the follow-up observations (in parentheses) ^b i -band PSF magnitudes with the Galactic extinction correction from the SDSS DR3 quasar catalog^c Image separations in units of arcsec between two components from the SDSS imaging data.^d Instruments (and filters) used for the follow-up observations. 8k: UH8k at UH88, QU: QUIRC at UH88, Op: Optic at UH88, WF: WFGS2 at UH88, Te: Tek2048 at UH88, DA: DIS III at ARC 3.5m, SP: SPIcam at ARC 3.5m, LR: LRIS at Keck, NR: NIRC at Keck, UF: UFTI at UKIRT, SC: Suprime-Cam at Subaru, MS: MMT spectrograph, EF: EFOSC2 at ESO 3.6m.

TABLE 4
LENSED QUASARS FROM THE SDSS DR3: STATISTICAL SAMPLE

Object	N_{img}	z^a	θ_{max}^b	f_i or f_I^c	Comment	Ref.
SDSS J0246–0825	2	1.682	1.04	0.34	SDSS lens	1
SDSS J0913+5259	2	1.377	1.14	0.70	known lens SBS 0909+523	2, 3
SDSS J0924+0219	4	1.524	1.78	0.43	SDSS lens	4
SDSS J1001+5027	2	1.838	2.86	0.72	SDSS lens	5
SDSS J1001+5553	2	1.405	6.17	0.94	known lens Q0957+561	3, 6
SDSS J1004+4112	5	1.732	14.62	0.23	SDSS lens	7, 8
SDSS J1021+4913	2	1.720	1.14	0.40	SDSS lens	9
SDSS J1226–0006	2	1.121	1.24	0.45	SDSS lens	10
SDSS J1332+0347	2	1.445	1.14	0.70	SDSS lens	11
SDSS J1335+0118	2	1.570	1.56	0.37	SDSS lens	12
SDSS J1524+4409	2	1.210	1.67	0.56	SDSS lens	13

REFERENCES. — (1) Inada et al. 2005; (2) Oscoz et al. 1997; (3) CASTLES webpage (C. S. Kochanek et al., <http://cfa-www.harvard.edu/castles/>); (4) Inada et al. 2003a; (5) Oguri et al. 2005; (6) Walsh et al. 1979; (7) Inada et al. 2003b; (8) Oguri et al. 2004a; (9) Pindor et al. 2006; (10) Inada et al. 2007b; (11) Morokuma et al. 2007; (12) Oguri et al. (2004b); (13) Oguri et al. 2007b.

^a Redshifts from the follow-up observations^b Maximum image separations in units of arcsec.^c Flux ratios between the brightest lensed image and the farthest lensed image from the brightest image, in the I - or i -band images.

TABLE 5
ADDITIONAL LENSED QUASARS IN THE SDSS DR3 QUASAR CATALOG

Object	N_{img}	z^a	θ^b	f_i or f_I^c	Comment	Reject ^d	Ref.
SDSS J0134–0931	5	2.216	0.68	0.03	known lens PMN J0134–0931	too small θ	1, 2, 3
SDSS J0145–0945	2	2.719	2.23	0.15	known lens Q0142–100	$z > 2.2, f_I < 10^{-0.5}$	3, 4
SDSS J0813+2545	4	1.500	0.91	0.06	known lens HS 0810+2554	by GALFIT fitting	3, 5
SDSS J0832+0404	2	1.115	1.98	0.22	SDSS lens	$f_I < 10^{-0.5}$	6
SDSS J0903+5028	2	3.584	2.80	0.46	SDSS lens	$z > 2.2$	7
SDSS J0911+0550	4	2.800	3.26	0.41	known lens RX J0911+0551	$z > 2.2$	3, 8
SDSS J1138+0314	4	2.442	1.44	0.35	SDSS lens	$z > 2.2$	3, 9
SDSS J1155+6346	2	2.890	1.83	0.50	SDSS lens	$z > 2.2$	3, 10
SDSS J1406+6126	2	2.126	1.98	0.58	SDSS lens	$i_{\text{cor}} > 19.1$	11
SDSS J1633+3134	2	1.511	0.66	0.30	known lens FBQ 1633+3134	$\theta < 1'', f_I < 10^{-0.5}$	12
SDSS J1650+4251	2	1.547	1.20	0.17	SDSS lens	by GALFIT fitting	13

REFERENCES. — (1) Winn et al. 2002; (2) Gregg et al. 2002; (3) CASTLES webpage (C. S. Kochanek et al., <http://cfa-www.harvard.edu/castles/>); (4) Surdej et al. 1987; (5) Reimers et al. 2002; (6) Oguri et al. 2007b; (7) Johnston et al. 2003; (8) Bade et al. 1997; (9) Burles et al. 2007; (10) Pindor et al. 2004; (11) Inada et al. 2007a; (12) Morgan et al. 2001; (13) Morgan et al. 2003.

NOTE. — See text for the selection of each lensed quasar.

^a Redshifts from follow-up observations.^b Maximum image separations in units of arcsec.^c Flux ratios between the brightest lensed image and the farthest lensed image from the brightest image, in the I - or i -band images.^d The reason that each lens is excluded from the statistical sample.